

## Efficiency of modern large-area photo-detectors

---

**Valentin Ivanov<sup>1</sup>**

*Institute of Computational Technologies, Siberian Branch of RAS*

*6, Acad. Lavrent'ev prosp., Novosibirsk, Russia*

*E-mail: vivanov.48@mail.ru*

The review of computational models and numerical results for end-to-end design of microchannel plate (MCP) amplifiers were presented. We use “microscopic” Monte Carlo (MC) simulations, empirical theories, and close comparison to experiment to obtain the influence of back-scattered electrons and the saturation effect on the emission properties of materials, in order to study the gain and transit times for various MCPs. We have applied this method to Al<sub>2</sub>O<sub>3</sub>, MgO emission materials of various thickness and surface quality. The experimental secondary emission yield (SEY) data were obtained at normal electron impacts and were used as the reference data for the adjustment of our MC simulations. The SEY at oblique angles of the primary electrons in the interval of 0 - 80° were calculated. The energy dependence of backscattered electron coefficients (BSC) for various primary electron incidence angles were calculated by MC for both materials and the results were compared to experimental “average” values obtained in the literature. Both SEY and BSC data were used for our “macroscopic” trajectory simulation that models of MCP amplifiers as whole devices, and is capable of gain and transit time calculations. The deposition and characterization experiments were conducted for the Large Area Picosecond Photodetector (LAPPD) project at Argonne National Laboratory.

*International Conference on New Photo-detectors - PhotoDet 2015*

*6-9 July, 2015*

*Moscow, Troitsk, Russia*

---

<sup>1</sup>Speaker

## 1. Introduction

Theoretical studies of secondary electron emission yields are necessary as a preliminary step of the development of new emission materials for MCP-based particle detectors in high-energy physics, such as Cherenkov's, neutrino, and astrophysical detectors [1,2]. Secondary electrons also play a significant role in the development of new scanning electron microscopes [3-13].

The goal of this work is to develop a parametrized set of the SEY dependencies in two variables, the energy of the primary electron (EPE) and the angle of incident electrons ( $\theta$ ), for  $\text{Al}_2\text{O}_3$  and  $\text{MgO}$  that are of interests for LAPPD collaboration. This parametrization can be done by using results obtained from Monte Carlo calculations with existing codes [5-7] modified to meet the needs of MCP developments, as well as by using the results of empirical SEY models [14-18]. The transit time values, gains and spatial resolution critical for the new large-area photo-detectors have not been available with the conventional glass MCPs [4]. Therefore, the new MCP concept is based on micron-scale pores fabricated in alumina by the tools developed in semiconductor industry.

## 2. Secondary electron emission and backscattered yields

The calculated SEY data were used as input files for a “macroscopic” MCP gain and transit time simulation that computes trajectories of multiple electrons inside an MCP. The feedback from the gain code was used to improve our understanding of the effect of MCP materials on device-level performance and to stimulate further search for better MCP materials.

Secondary electron emission is an important tool for surface microanalysis in various research, science, and industrial areas. Primary electron collisions with the surface of a target generate emissions of various types of secondary electrons [10].

The total number  $\delta$  of emitted secondary electrons per primary electron is the number of electrons emitted with high energies [5]. The materials constants,  $\epsilon$ , the average energy necessary to produce one secondary electron and  $\lambda$ , the electron escape length tuned to obtain the best fit of the SEY experimental data for electrons at normal incidence are provided in Table 1. Here we obtained the data for  $\text{Al}_2\text{O}_3$  and  $\text{MgO}$  by direct MC calculations, where the adjustable parameters were obtained from publications [7,8].

Table 1. Material properties

Material	$\epsilon$ , eV	$\lambda$ , Å
$\text{Al}_2\text{O}_3$	27.5	20
$\text{MgO}$	20	120

Data for the normal incidence, 45 and 80 degrees of incident angles shown in Fig. 1 were chosen to match the input used by “CASCADE”, an MCP simulation developed at the

Arradiance company [19]. Our MC simulations of SEY for  $\text{Al}_2\text{O}_3$ , with the parameters in Table 1, were close to the “CASCADE” results at normal incidence. However, we did not try to simulate the SEY at oblique incident angles  $10\text{-}80^\circ$  due to a vast choice of the simulation parameters to fit. Instead, we used an empirical formula that has an excellent fit for all simulated angles [6]:

$$\delta/\delta_m = 1.11(E/E_m)^{-a} \left[ 1 - \exp\{-2.3(E/E_m)^b\} \right], \quad (1)$$

where  $a = 0.225$ ,  $b = 1$  were obtained to give the best fit to the “CASCADE” curves for the angles in the interval of  $0\text{-}80^\circ$ . Figure 1 (left) shows the secondary emission yield generated by primary electrons with energies of  $E = 0\text{-}800$  eV and incident angles in the range of  $0^\circ \leq \theta_i \leq 80^\circ$  bombarding an  $\text{Al}_2\text{O}_3$  substrate.

The values of  $\delta_m$ ,  $E_m$  at various incidence angles were obtained by a smooth interpolation of the appropriate SEY and  $E$  values for the “CASCADE” yields.

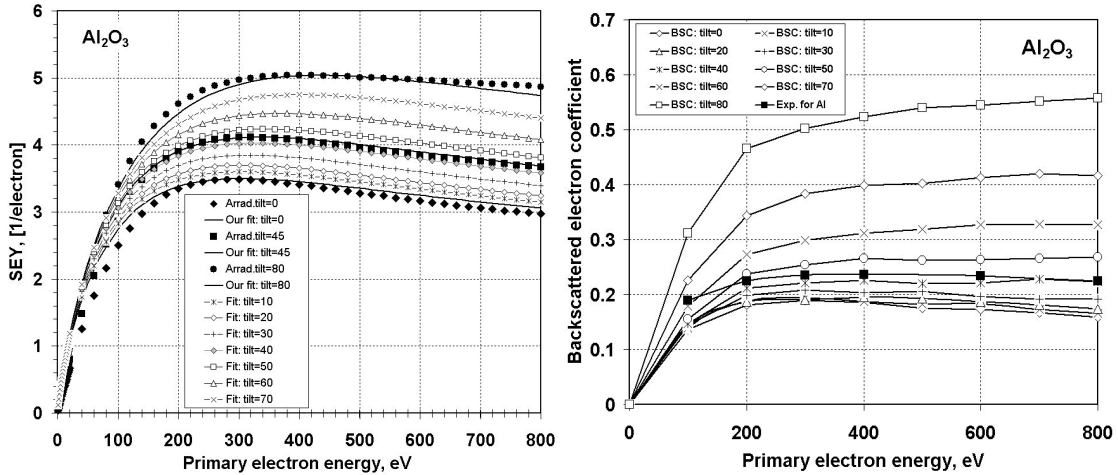


Figure 1. Left: Fitting the secondary emission yields of  $\text{Al}_2\text{O}_3$  at different primary electron incoming angles. Right: Energy dependence of  $\text{Al}_2\text{O}_3$  backscattered electron coefficients at different electron incoming angles. Solid symbols are experimental values for pure Al [8].

Figure 1 (right) shows the energy dependence of  $\text{Al}_2\text{O}_3$  backscattered electron coefficients for oblique electron incoming angles obtained by a Casino code [21]. Figure 2 shows the energy and angular dependences of SEY and backscattered electron coefficients (BSC) of electrons for MgO at various incident angles in the interval  $0 \leq \theta_i \leq 80^\circ$  simulated by a MC code [5,7].

The parametrized data shown in Fig. 1-2 were then submitted as input data for a Monte Carlo trajectory code that models the whole MCP device.

Since the charging of highly resistive ceramics gives incorrect SEY results, it is important to compare the experimental measurements with the  $\text{Al}_2\text{O}_3$  emission.

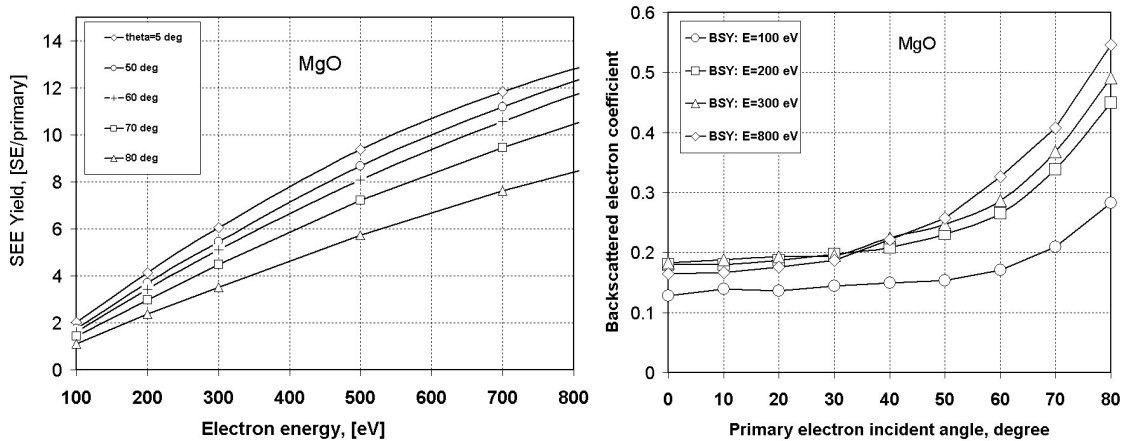


Figure 2. Left: Energy dependence of MgO secondary emission yields (SEY) calculated by a Monte Carlo method for different primary electron incoming angles and different primary electron energies. Right: Energy dependence of MgO backscattered electron coefficients at different electron incoming angles.

### 3. MCP gain and transit time simulations

Here we present the results of numerical simulation using our code “MCS” (Monte Carlo Simulator) that takes into account saturation effect [22], and compare them with the results obtained by the code “CASCADE”. The initial data set includes a single plate of 1.2 mm thickness with 20  $\mu\text{m}$  pores, 8° bias angle, and 1 kV applied voltage. The energy of incoming photo electrons is 350 eV, the single electrons travel in the pores to the exit with a number of collisions, and create the cascades of secondaries. Then we calculate the gain factor for each cascade of secondary electrons and arrival time (AT), defined as the time when the MCP pulse crosses 10% of the pulse maximum, for each pulse, and average those parameters over the number  $N$  of input signal pulses.

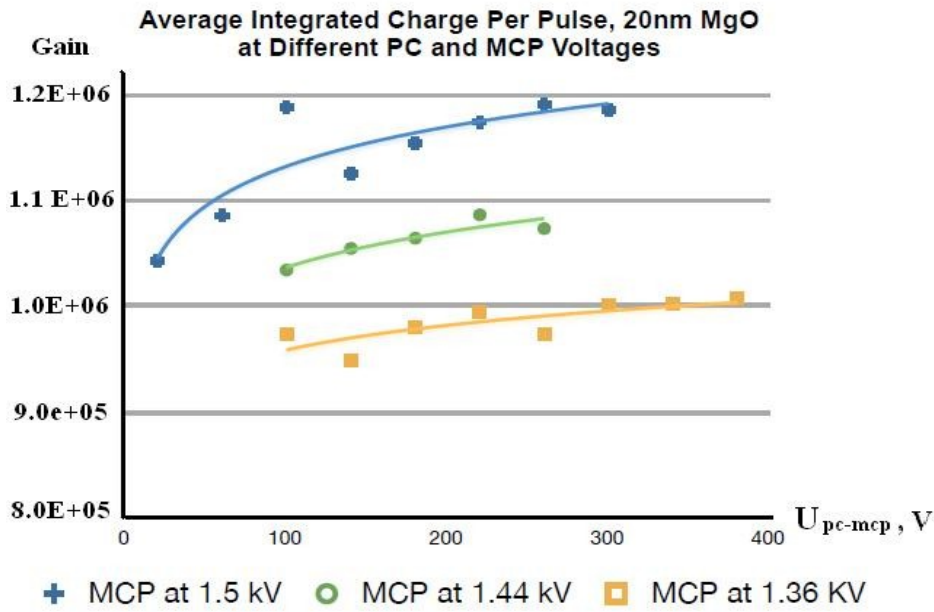


Figure 3. Averaged gain at different voltages for photo cathode and MCP. Solid lines – numerical simulations, dots – experimental data.

The numerical results show that back-scattering phenomena should have a significant impact on the gain and a discernible effect on the transit time of the MCPs. This was important for comparison of the device-level MCP measurements with “MCS” simulations for different materials. Figure 3 demonstrates a good agreement for the averaged gain factor for numerical and experimental data at different photo cathode and MCP voltages. Time-profile for the pulse at the MCP exit, and the pulse-height distributions were obtained by two different codes are shown in Figure 4.

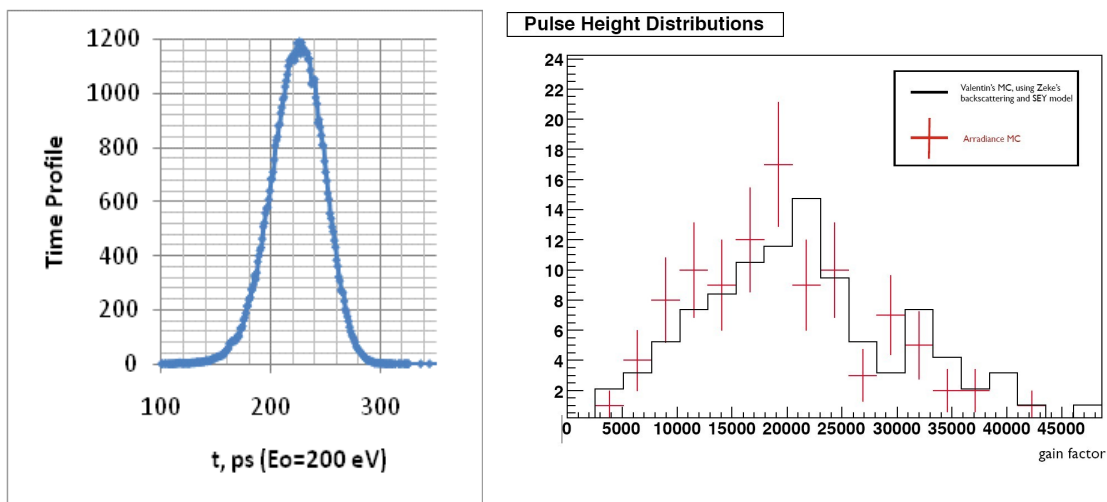


Figure 4. Time profile for the pulse on the MCP exit (left), and comparison of pulse-height distributions obtained by the “MCS” (solid line) and “CASCADE” (red cross) codes shows a good agreement (right).

#### 4. Charge relaxation time computation

ZnO/Al<sub>2</sub>O<sub>3</sub> alloy films were fabricated by using atomic layer deposition (ALD) techniques. By adjusting the ALD pulse sequence, the ZnO/Al<sub>2</sub>O<sub>3</sub> alloy film composition was varied from 0% to 100% ZnO [10]. The material constants and physical properties of these alloy films, such as surface roughness, resistivity, dielectric constants, and film thickness were selected so that these materials could be used as resistive and emission layers in large-area photo detecting MCPs, as compared with conventional glass substrates. Charge relaxation and gain depletion mechanisms, effects of a strong electric field, and geometry parameters of the coating for large-area fast photo detectors were discussed in [23].

A new ambipolar solid state plasma drift-diffusion model of the charge relaxation in such materials as ZnO/ Al<sub>2</sub>O<sub>3</sub> in various combination of the content was proposed. It includes the generation of electrons and holes via impact ionization due to acceleration in a strong electric field [24]. Some of the equations of this model are given in [25-28].

1. The following conductivity of AZO film with 20% Al was used:  $\mu = 10^7$  ( $\Omega$  cm). The diffusion coefficients of amorphous alumina are unknown. Therefore, we used the diffusion coefficients of alumina via alumina carrier mobility that are given for some limited mixture content in Ref. [29]. Assuming linear dependence between conductivity and mobility, the mobility of a mixture Al<sub>2</sub>O<sub>3</sub>+ZnO was extrapolated from low to high Al content. The results of our calculations shown at Figure 5 were compared with the results of a simple Maxwell relaxation time model and with the circuit charge relaxation model developed for the MCP device [30].

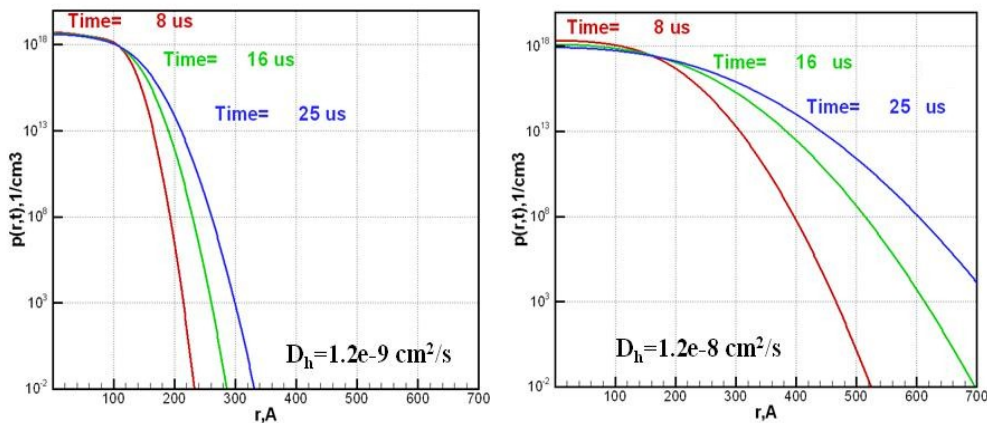


Figure. 5. Results of our calculation with the drift-diffusion model in spherical geometry, with two different diffusion coefficients  $D_h$ .

## 5. Conclusions

The developed physical models, numerical algorithms and computer codes allowed to provide the end-to-end design for large-area photo-detector of picosecond timing resolution, to optimize the device parameters, and considerably reduce the period of the development. Further experimental data show a good agreement with our simulation results.

## References

- [1] E. Nappi, *Advances in the photodetection technologies for Cherenkov imaging applications*, Nucl. Instr. Meth. A 604 (2009) 190-192.
- [2] S.M. Bradbury *et al.*, *Test of the new hybrid INTEVAC intensified photocell for the use in air Cherenkov telescopes*, Nucl. Instr. Meth. A387 (1997) 45-49.
- [3] D.R. Beaulieu *et al.*, *Novel microchannel plate device fabricated with atomic layer deposition*, AVS Topical Conf. on Atomic Layer Deposition, ALD 2009, Monterey, CA, July 19-22, 2009.
- [4] J.A. Anderson *et al.*, *New developments in fast-sampling analog readout of MCP based large-area picosecond time -of-flight detectors*, IEEE-MIC 2008, ID-2973.
- [5] D.C. Joy, *Monte Carlo modeling for electron microscopy and microanalysis*, Oxford Univ. Press, 1995.
- [6] D.C. Joy, *A model for calculating secondary and backscattering electron yields*, J. Microscopy, 147 (1987) 51-64.
- [7] D.C. Joy, *private communication*, 2009.
- [8] I.M. Bronstein, B.S. Fraiman, *Secondary electron emission*, Nauka-Moscow, 1969.
- [9] K. Kanaya, S. Ono, F. Ishigaki, *Secondary electron emission from insulators*, J. Phys. D 11 (1978) 2425-2437.
- [10] H. Seiler, *Secondary electron emission in the scanning electron microscope*, J. Appl. Phys. 54 (1983) R1-R18.
- [11] J.R. Young, *Penetration of electrons in Al<sub>2</sub>O<sub>3</sub>-films*, Phys. Rev. 103 (1956) 292-293.
- [12] R.O. Lane, D.I. Zaffarano, *Transmission of 0-40 keV electrons by thin films with application to beta-ray spectroscopy*, Phys. Rev. 94 (1954) 960-964.
- [13] K. Ohya, I. Mori, *Influence of backscattered particles on angular dependence of secondary electron emission from Copper*, J. Phys. Soc. Jpn. 59 (1990) 1506-1517.
- [14] M. Ito, H. Kume, K. Oba, *Computer analysis of the timing properties in micro channel plate photomultiplier tubes*, IEEE Trans. NS-31 (1984) 408-412.
- [15] A.J. Guest, *A computer model of channel multiplier plate performance*, Acta Electronica, 14 (1971) pp.79-97.
- [16] M. Baroody, *A theory of secondary emission from metals*, Phys. Rev. 78 (1950) 780-787.
- [17] R.G. Lye, A.J. Dekker, *Theory of secondary emission*, Phys. Rev. 107 (1957) 977-981.
- [18] B.K. Agarwal, *Variation of secondary emission with primary electron energy*, Proc. Phys. Soc. 71 (1958) 851-852.

- [19] “CASCADE” code ([www.arradiance.com](http://www.arradiance.com)).
- [20] A.L. Pregoner, *Monte Carlo calculations of low energy electron backscatter coefficients*, Nucl. Inst. Meth. B6 (1985) 562-565.
- [21] P. Hovington et al., *CASINO: A new Monte Carlo code in c Language for electron beam interaction*, Scanning 19 (1997) 1-14.
- [22] V. Ivanov, Z. Insepov, *Gain and Time Resolution Simulations in Saturated MCP Pores*, NIM A, 52549 (2010) 02291-6.
- [23] A. K. Jonscher, *Principles of semiconductor device operations*, Wiley (1960).
- [24] A. G. Chynoweth, J. Appl. Phys. 31 (1960) 1161-1165.
- [25] A. H. Marshak, Proc. IEEE 72 (1984) 148-164.
- [26] R. Van Overstraeten, Solid St. Electronics 13 (1970) 583-608.
- [27] L.M. Biberman, Proc. IEEE 59 (1972) 555-572.
- [28] Z. Insepov et al., Phys. Rev. A77 (2008) 062901.
- [29] F. Ruske et al., J. Appl. Phys. 107 (2010) 013708.
- [30] A. B. Berkin, V. V. Vasil'yev, Techn. Phys. Lett. 33 (2007) 664-666.